Swelling of phospholipids by monovalent salt

Horia I. Petrache,[1,*] Stephanie Tristram-Nagle,[†] Daniel Harries,[*] Norbert Kučerka,[†] John F. Nagle,[†,§] and V. Adrian Parsegian[*]

Laboratory of Physical and Structural Biology,* National Institute of Child Health and Human Development, National Institutes of Health, Bethesda, MD 20892-0924; and Biological Physics Group, Department of Physics,[†] and Department of Biological Sciences,[§] Carnegie Mellon University, Pittsburgh, PA 15213

Abstract Critical to biological processes such as membrane fusion and secretion, ion-lipid interactions at the membrane-water interface still raise many unanswered questions. Using reconstituted phosphatidylcholine membranes, we confirm here that multilamellar vesicles swell in salt solutions, a direct indication that salt modifies the interactions between neighboring membranes. By varying sample histories, and by comparing with data from ion carrier-containing bilayers, we eliminate the possibility that swelling is an equilibration artifact. Although both attractive and repulsive forces could be modified by salt, we show experimentally that swelling is driven primarily by weakening of the van der Waals attraction. To isolate the effect of salt on van der Waals interactions, we focus on high salt concentrations at which any possible electrostatic interactions are screened. By analysis of X-ray diffraction data, we show that salt does not alter membrane structure or bending rigidity, eliminating the possibility that repulsive fluctuation forces change with salt. By measuring changes in interbilayer separation with applied osmotic stress, we have determined, using the standard paradigm for bilayer interactions, that 1 M concentrations of KBr or KCl decrease the van der Waals strength by 50%. By weakening van der Waals attractions, salt increases energy barriers to membrane contact, possibly affecting cellular communication and biological signaling.— Petrache, H. I., S. Tristram-Nagle, D. Harries, N. Kučerka, J. F. Nagle, and V. A. Parsegian. **Swelling of phospholipids by monovalent salt. *J. Lipid Res.* 2006.** 47: **302–309.**

Supplementary key words bending rigidity • halides • hydration • ion binding • lipid head group • membrane interactions • solvation

From bacteria to mammals, biological processes take place in salt solutions. Maintaining a delicate balance of ions, biomembranes interact preferentially with different ionic species (1). Specific ionic effects have been shown to influence the growth rates of bacteria (2) and fungi (3, 4) and to affect the function of antibiotic channels (5). This investigation will focus on the halide salts because of their presence in intracellular and intercellular fluids. At biomembrane surfaces, halides encounter not only charged lipid species, such as phosphatidylserine and phosphatidylinositol, but more often common neutral phosphatidylcholines (PCs). Interactions with both types of lipids require investigation: by affecting lipid interactions, salt solutions modulate biological processes such as fusion and secretion.

Despite being electrically neutral, PC membranes attract one another as a result of mutually induced charge fluctuations (6). Because of different dielectric properties of membranes and the intervening solvent, transient spontaneous electromagnetic fields in one membrane induce correlated fields in the neighboring membrane and vice versa, resulting in an attractive force. This "charge fluctuation" (van der Waals) force is responsible for the spontaneous formation of stable multilamellar structures [e.g., myelin sheets in vivo and multilamellar vesicles (MLVs) in vitro]. When the attractive van der Waals force is exactly balanced by repulsive forces, an equilibrium spacing between lamellae is established (6–9). Typically, as measured by small-angle X-ray scattering, the interlamellar spacing of neutral membranes in water is on the order of the membrane thickness itself. However, membrane spacings depend sensitively on the nature of the solvent (7, 10, 11). Therefore, any alteration of the repeat spacing with solvent composition is an indication of a shift in the balance of attractive and repulsive forces between membranes. Here, we specifically address the modification of interbilayer forces by monovalent salt.

Modification of interbilayer forces by solvents and solutes, including monovalent salt, has been recognized in the past (7, 10, 12–16). However, outstanding questions remain: What is the swelling mechanism? What is the nature of ionic specificity? Does salt affect membrane structure in addition to interactions? With recent advances in X-ray methods for the determination of bilayer structure and interactions (17–19), we are now in a position to address salt effects on multilamellar lipid structures. Significant ion-lipid interactions are expected not only because of dielectric gradients across the biomembrane interface but also because of the dipolar nature of head groups. Ion-lipid interactions have been measured by solid-state NMR

Manuscript received 8 September 2005 and in revised form 1 November 2005.

Published, JLR Papers in Press, November 2, 2005.
DOI 10.1194/jlr.M500401-JLR200

[1] To whom correspondence should be addressed.
e-mail: petrachh@mail.nih.gov

spectroscopy (20), electrophoretic mobility (21–23), and monolayer surface pressure (24). The electrostatic nature of ion-lipid interactions has raised experimental questions as well, highlighting possible equilibration complications, such as the case of Li salts (25) or high-temperature melting lipids (26).

Here, we show that the swelling of PC bilayers by monovalent salt is driven mainly by the weakening of van der Waals attractive forces through screening of charge fluctuations. MLVs swell more in the presence of Br^- compared with Cl^- as a result of a higher propensity of bromine ions to associate with the polar lipid head groups (22, 27–31), causing an added electrostatic repulsion between the now charged surfaces. To isolate the effect of salt on van der Waals interactions, we focus on interbilayer forces in the presence of high salt concentrations at which the strongly screened electrostatic interaction can be neglected. Finding that the bilayer structure and bending rigidity are practically unaffected by salt, we obtain excellent fits to osmotic pressure data at high salt with empirically determined interaction parameters. We conclude that ions must regulate biomembrane interactions not only through electrostatic interactions but also by a significant screening of charge fluctuations. By decreasing biomembrane adhesion energy, ionic action at the biomembrane interface presents a probable regulatory mechanism for exocytosis, endocytosis, synaptic transmission, fertilization, and viral infection.

MATERIALS AND METHODS

Highly purified (>99%) synthetic 1,2-dicapryl-*sn*-glycero-phosphatidylcholine, 1,2-dilauroyl-*sn*-glycero-phosphatidylcholine (DLPC), 1,2-dimyristoyl-*sn*-glycero-phosphatidylcholine (DMPC), and 1,2-dioleoyl-*sn*-glycero-phosphatidylcholine (DOPC) were purchased from Avanti Polar Lipids (Alabaster, AL) and used without further purification. Organic solvents were high-performance liquid chromatography grade from Aldrich (Milwaukee, WI). KCl and KBr salts of purity >99% were from Sigma-Aldrich (St. Louis, MO).

MLV (unoriented) samples

Lyophilized lipids were hydrated with purified water or salt solutions. When osmotic pressure was applied, the hydrating solution included high molecular weight polyethylene glycol (20,000) or dextran (500,000) of known concentrations. Samples were cycled below and above the chain melting transition temperatures, occasionally vortexed or shaken, and then typically stored for >48 h at 4°C. Variations in protocol included a 48 h room temperature storage with or without vortexing or shaking to test the dependence of sample history on equilibration. No differences were detected. Before being exposed to X-ray for 30–60 min with a fine-focus fixed Cu anode X-ray source, samples were allowed to thermally equilibrate between 1 h and 7 days. No differences in the quality of the spectra or scattering peak position were observed. Sharp, uniform scattering rings were obtained indicative of sample homogeneity upon equilibration (full width at half maximum 0.01–0.03 $Å^{-1}$). Lattice spacings were recorded as a function of applied osmotic pressure.

Oriented samples

Oriented samples were studied as described recently by Kučerka et al. (19). The main difference was that salt was added to the organic solvent from which the oriented samples were prepared using the rock-and-roll method (32). The amount of salt that was added was adjusted so that the concentration of salt in the interlamellar water space at full hydration equaled that of the MLVs. X-ray data for oriented samples were taken at the D-1 station of the Cornell High-Energy Synchrotron Source using the sample chamber and following the procedures described by Kučerka et al. (19).

After correcting for absorption and the Lorentz factor, the scattering intensity I(q) is given by the standard relation (33):

$$I(q) = |F(q_z)|^2 S(q) \qquad (Eq.\ 1)$$

We first obtain S(q) (the structure factor) and then divide into I(q) to obtain $|F(q_z)|^2$. The bilayer form factor $|F(q_z)|$ is the usual transformation of the electron density $\rho(z)$ across a single bilayer immersed in water with the fluid electron density ρ_W subtracted. Our method for obtaining S(q) was developed previously and applied to DOPC (18, 34), DLPC (19), and DMPC (19). The smectic liquid crystal theory is fit to the decay of the diffuse scattering in the q_r direction to obtain K_C, the bending modulus, and B, the compression modulus; these are the fundamental material parameters that determine the fluctuations and allow the calculation of S(q). The $|F(q_z)|$ is corrected for a geometric distortion caused by the undulation fluctuations (9) and fit to the hybrid model of the electron density profile (35). F(0) is obtained from the following equation (36, 37):

$$AF(0) = 2(n_L - V_L\rho_W) \qquad (Eq.\ 2)$$

where the number of electrons n_L is 342 for DLPC, the electron density of water is $\rho_W = 0.333\ e/Å^3$, and the volume of the lipid V_L is 991 $Å^3$ for DLPC using the neutral flotation method (38, 39). In the case of DLPC with salt, the concentration of the interlamellar solvent was measured, and the densities at 30°C were researched (40, 41). The electron densities of salt water were $0.345\ e/Å^3$ for DLPC with 0.875 M interlamellar KCl (vs. 1 M bulk) and $0.336\ e/Å^3$ for DLPC with 0.025 M interlamellar KBr (vs. 0.1 M bulk). The area (A)/lipid, bilayer thickness, and water/lipid are some parameters that are obtained from the model fit (19).

RESULTS

Salt-induced swelling

Interlamellar repeat spacings for the 12 carbon DLPC in KCl and KBr aqueous solutions at 25°C are shown in **Fig. 1** as functions of salt concentration. To emphasize the qualitative change of scattering peaks with salt, we also show representative X-ray spectra. Scattering peaks become very broad in high salt (Fig. 1D), making assignment of peak position difficult, thereby limiting D-spacing data to salt concentrations of <3 M for KCl and <2 M for KBr. From an equilibrium distance of ~58 Å in pure water, DLPC multilayers swell progressively with added salt, reaching an apparent limiting value of 75 Å for KBr, whereas the maximum measurable value for KCl is 68 Å. The 12 carbon DLPC lipid is not a special case. Other PC lipids with different chain lengths also swell with monovalent salt, as shown in **Fig. 2**. Figure 2A shows the directly measured

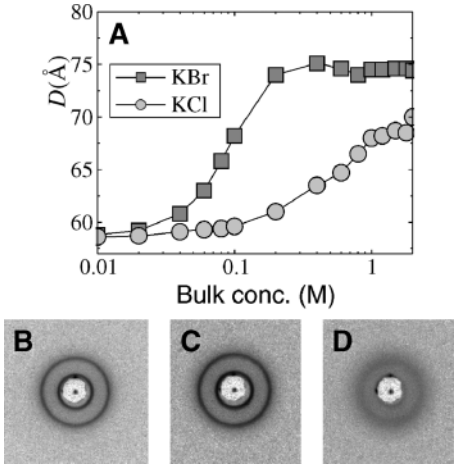

Fig. 1. A: X-ray D-spacings versus bulk salt concentration from fully hydrated unoriented multilamellar 1,2-dilauroyl-*sn*-glycero-phosphatidylcholine (DLPC) bilayers at 25°C. Primary X-ray data for the first two orders are shown as dark rings for water (B), 100 mM KCl (C), and 100 mM KBr (D) at 25°C.

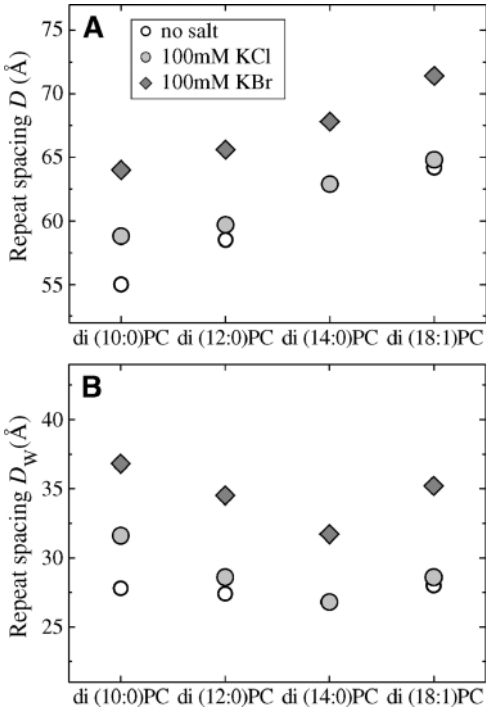

Fig. 2. Repeat spacing (A) and Luzzati water thickness (B) upon adding 0.1 M KCl or KBr to the fluid states (35°C) of 1,2-dicapryl-*sn*-glycero-phosphatidylcholine [di(10:0)PC], DLPC [di(12:0)PC], 1,2-dimyristoyl-*sn*-glycero-phosphatidylcholine (DMPC) [di(14:0)PC], and 1,2-dioleoyl-*sn*-glycero-phosphatidylcholine (DOPC) [di(18:1)PC]. By subtracting Luzzati membrane thicknesses (9, 19, 42) from the D-spacings, comparison of the resulting water spacings in B shows that swelling with salt is strengthened by either decreasing the chain length from 14 to 10 carbons per chain or by introducing a single double bond into each chain.

repeat spacing D, whereas Fig. 2B shows only the variation of interlamellar water spacing $D_W = D - D_B$, obtained by subtracting the chain length-dependent bilayer thicknesses D_B (9, 19, 42). Although a revised definition for the membrane thickness is used later for the analysis of membrane interactions (see below), for easy comparison with the literature, Fig. 2B uses the more common Luzzati definition that equates D_B with the ratio of lipid volume and lipid cross-sectional area. Relative to DMPC, Fig. 2B shows an increase in water spacings either with decreasing numbers of carbons per hydrocarbon chain or with the introduction of double bonds.

Equilibration (dismissing an old myth)

One concern is that multilamellar structures might not fully equilibrate in salt solutions because lipid membranes have low permeability to ions, thereby precluding access to the inner water layers in MLVs. In fact, preparation of unilamellar vesicles often relies upon this property: liposomes are metastable states of salt-filled vesicles (43). Salt gradients form as a result of freeze-thawing and extrusion. However, in our experiments, it is clear that salt does enter the inner water layers of MLVs; otherwise, external salt would impose an osmotic pressure that tends to reduce the water spacing in contrast with the observed swelling. Our experience with fluid, thin membranes (such as DLPC) is that equilibration, as measured by X-ray D-spacing, is fast, reaching stability within minutes. Samples incubated at 4°C for >12 h, then exposed to X-ray for 30 min at 35°C without preequilibration, showed no trace of the lower temperature D-spacing. (With our setup, it takes <3 min for the sample holder to equilibrate at the new temperature.) Reversibility is also robust. Fast equilibration occurs for oriented samples as well. This suggests that ions (and water) flow through inherent defect regions of multilamellar stacks. Additional equilibration measurements were done in the presence of the common ionophores amphotericin B, nystatin, and valinomycin. No changes in interlamellar spacings or equilibration times were detected for ionophore contents of <0.5% by weight. Changes were indeed seen at higher ionophore contents, but those are attributable to permanent alteration of membrane structure and interactions rather than to changes in equilibration times. Finally, the most compelling argument that our samples are not trapped in local energy minima is reproducibility. We measured multiple sample batches with diverse histories and always obtained the same results.

Bilayer structure and stiffness do not change with added salt

To determine whether salt affects membrane structure and mechanical properties, we have focused on oriented DLPC multilayers. **Figure 3** shows the diffuse scattering from an oriented sample of DLPC close to full hydration. The absolute values of the continuous form factors $|F(q_z)|$ are plotted in **Fig. 4A** for DLPC, DLPC/1 M KCl, and DLPC/0.1 M KBr at 30°C. These two salt concentrations were chosen to have the same lamellar D-spacing as indicated in Fig. 1. There are small but noticeable differences among the $|F(q_z)|$ for the three samples, which suggest that

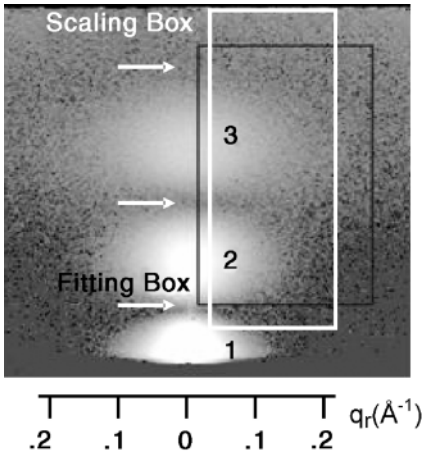

Fig. 3. Diffuse scattering data from an oriented sample of DLPC with added KBr. High intensity is shown as white on a black background. There are three lobes of diffuse scattering, numbered 1–3, separated by zeros in intensity (shown by arrows) that clearly determine reversal in the phase of the form factor F(q) as a function of scattering angle. The fit to the Caillé theory (see Materials and Methods) was made in the black fitting box, and the scaling factor to obtain structural parameters was obtained from the data in the white scaling box. The vertical axis is in the q_z lamellar scattering direction. The gray scale is chosen to emphasize the diffuse scattering, so the very intense and sharp h = 1 and h = 2 lamellar peaks that occur in the first lobe are not seen here.

the bilayer structure is different in different salt solutions. However, the electron density profiles in Fig. 4B that were obtained from these F(q) values show that the bilayer structures are virtually identical. The differences in the F(q) values are attributable to differences in the electron density of the interlamellar water region resulting from the addition of salt. This changes slightly the electron density contrast between lipids and salt solutions without apparently changing the electron density of the bilayers.

To obtain the continuous form factors and the absolute electron density profiles, we necessarily obtain the membrane bending rigidity K_C and the stacking compressibility B, which is a composite measure of hydration forces, van der Waals forces, and the fluctuation force. The K_C values are plotted in **Fig. 5A** as a function of D-spacing for all three samples at 30°C. These values do not vary significantly with salt or D-spacing. The average values are included in **Table 1**. In contrast, the compression modulus B does vary as a function of D-spacing (44, 45). These values are plotted in Fig. 5B. Data points from all three samples are consistent with a log-linear fit as shown.

Effect of osmotic pressure on swelling with and without salt

The single most important determinant of interactions between bilayers is obtained by imposing osmotic pressure P and measuring water spacing a to obtain P(a) data (6). Here, we have chosen to define a as the steric water spacing $a = D - D_B'$, where D_B' is the steric thickness of the bilayer instead of the Luzzati thickness. At low osmotic pressures, $D_B' = 39$ Å at 30°C from the DLPC structure determination (19). For high osmotic pressures, the standard correction to membrane thickness (6) was applied using an areal compressibility $K_A = 250$ dyn/cm (46). **Figure 6** shows our P(a) data for MLVs of DLPC with no salt and with 1 M KCl and 1 M KBr.

Analysis

The currently accepted framework of interbilayer interactions for uncharged fluid phase membranes involves a van der Waals attractive force and two repulsive forces: hydration and bending fluctuations. Although the attractive van der Waals force can be calculated analytically for a pair of infinitely extended slabs of thickness b (47), the repulsive forces are typically described phenomenologically

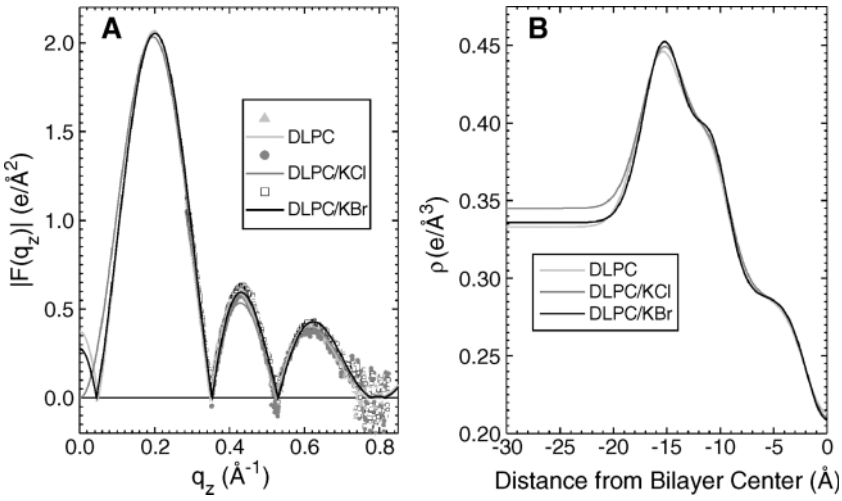

Fig. 4. A: Absolute values of continuous form factors: symbols are data and lines are model fit to the data. Negative values indicate statistical fluctuations when the form factors are close to zero. B: Electron density profiles of DLPC, DLPC/1 M (bulk) KCl, and DLPC/0.1 M (bulk) KBr at 30°C. Half of the bilayer is shown. Note the difference in electron densities of the different solvents that accounts for most of the differences in the form factors in A.

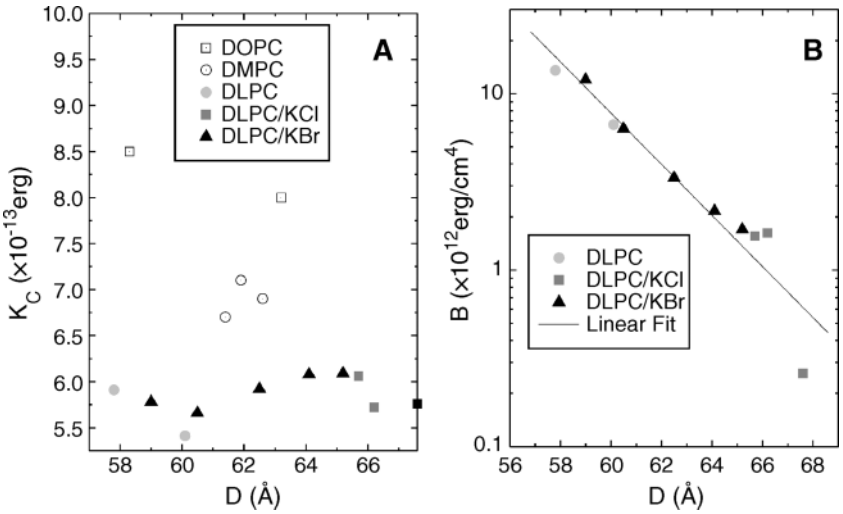

Fig. 5. Values of the bending modulus K_C (A) and the compression modulus B (B) obtained from DLPC (light gray circles), DLPC/1 M bulk KCl (gray squares), and DLPC/0.1 M bulk KBr (black triangles) at 30°C. K_C values for DOPC (open squares) and DMPC (open circles) are shown for comparison. The linear fit to log B is consistent with the exponential form of the fluctuation force in equation 3, and its slope is related to the decay length λ_{fl} using equation 4.

through empirically determined parameters and functional forms. Equation 3 shows this decomposition of interbilayer interactions (45):

$$P(a,T) = -\frac{H}{6\pi}\left(\frac{1}{a^3} - \frac{2}{(a+b)^3} + \frac{1}{(a+2b)^3}\right) + P_h e^{-a/\lambda_h} + \left(\frac{k_B T}{2\pi}\right)^2 \frac{1}{K_C}\frac{A_{fl}}{\lambda_{fl}} e^{-a/\lambda_{fl}} \qquad (Eq.\ 3)$$

The first term represents the van der Waals attraction with an interaction strength given by the Hamaker parameter (H), and we use $b = D_B'$ as defined above. The second term represents the hydration force, accounting for the energetic cost of water ordering in the vicinity of lipid head groups. This force is exponential, with a decay length $\lambda_h \sim 2$Å (6, 16, 45). It dominates the total interbilayer force for small water spacings and becomes increasingly less significant for interbilayer spacings >10 Å. The third term in equation 3 is the shape fluctuation or undulation term, which becomes the dominant repulsive term at larger water spacings (8). It accounts for the entropic penalty attributable to the confinement of undulating membranes (48). This entropic force is inversely proportional to the bilayer bending rigidity, K_C. The scale factors P_h and A_{fl} depend sensitively on the choice of membrane thickness as described above, but once that choice is made, they should be invariant unless the strength of these repulsive interactions changes.

Figure 6 shows that the effect of salt is significant at low osmotic pressure but becomes small at high osmotic pressure, at which the dominant force between bilayers is the hydration force. Therefore, Fig. 6 suggests that salt affects the hydration force in a relatively minor way. This is not a simple conclusion, because the concentration of salt likely decreases to zero as the water spacing becomes small. However, the hydration force is inconsequential for large separations, so in the regime in which salt is important, other interactions must be affected. Therefore, we obtain the best values of P_h and λ_h to fit the high osmotic pressure

TABLE 1. Values of parameters for 1,2-dilauroyl-*sn*-glycerophosphatidylcholine bilayer samples that are used in equation 1 to provide the theoretical lines in Fig. 6.

Parameter	No Salt	1 M KCl	1 M KBr
P_h (10^9dyn/cm^2)	1.6 ± 0.2	2.2	2.8
λ_h (Å)	2.1 ± 0.1	2.2	2.2
K_C (10^{-13}ergs)	5.8 ± 0.2	5.8	5.8
A_{fl} (Å^{-2})	1.06 ± 0.10	1.06	1.06
λ_{fl} (Å)	6.0 ± 0.2	6.0	6.0
H (10^{-14} ergs)	9.2 ± 0.5	5.0	3.8

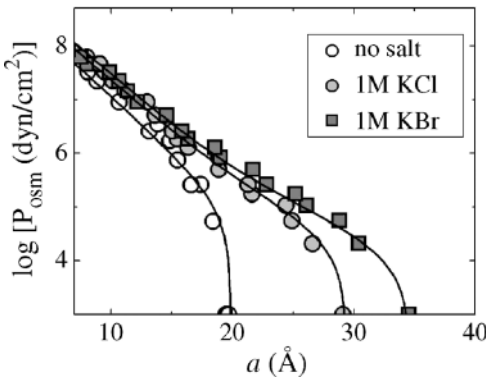

Fig. 6. Each symbol shows the experimental value of the osmotic pressure (P_{osm}) that was fixed for each unoriented multilamellar DLPC sample versus the water spacing (a) that was determined for that sample as the D-spacing minus the steric bilayer thickness. The lines show the fits to these data using equation 3. The fitted parameters in equation 3 are shown in Table 1. All data were taken at 25°C.

data for all three solutions and fix them to the values shown in Table 1 in the subsequent fitting.

The results shown in Fig. 5 provide important information about the fluctuation forces in the fit. First, we recall (45) that the B modulus is given by

$$B(a) = \left(\frac{k_B T}{2\pi}\right)^2 \frac{1}{K_C \sigma^4} = \left(\frac{k_B T}{2\pi}\right)^2 \frac{1}{K_C} A_{fl}^2 \exp(-2a/\lambda_{fl}) \quad (Eq.\ 4)$$

where σ represents the root mean square fluctuation of the nearest neighbor spacings. The experimental results that K_C is the same and that the B values fall on the same curve in Fig. 5B imply that the parameters λ_{fl} and A_{fl} for the repulsive fluctuation force should be the same for all three solutions. Furthermore, the fit to the $B(a)$ data shown in Fig. 5B provides the parameters λ_{fl} and A_{fl} as shown in Table 1. Therefore, within the standard paradigm of equation 3, the only remaining parameter that can account for the swelling of D with salt is the Hamaker parameter H of the attractive van der Waals interaction. Table 1 shows the values of H that were obtained by fitting all of the osmotic pressure $P(a)$ data while holding the other parameters fixed to the values obtained as described above. The fits to the $P(a)$ data are shown in Fig. 6.

DISCUSSION

Our structural results in Fig. 4B show that salt has negligible effects on the thickness of DLPC bilayers. Therefore, the main reason for the swelling of multilamellar arrays with added salt shown in Fig. 1A is swelling of the water space between the bilayers. Consistent with the invariance of bilayer structure, the measured bilayer rigidity K_C in Fig. 5A also does not change with added salt.

Because interbilayer forces arise from complicated many-body interactions, the simplified phenomenological model embodied in equation 3 has been used as the basis for interpretation of our experimental results. We have experimentally determined interbilayer interaction parameters by measuring the osmotic pressure curves (Fig. 6), the membrane bending rigidity (Fig. 5A), and the stacking-compression parameter B (Fig. 5B) versus interlamellar spacing. Importantly, and not obvious a priori, within experimental uncertainty the variation of B with interlamellar spacing is unaffected by salt, indicating that fluctuation parameters are not affected. Within the context of equation 3, it is clear that a change of the Hamaker parameter is needed to fit the osmotic pressure data in Fig. 6. Table 1 shows the values of all parameters. This table emphasizes that the Hamaker parameter is substantially reduced when salt is added to multilamellar arrays. This is a direct experimental proof of the theoretical expectation (47, 49) used by Korreman and Posselt (10) to interpret their salt-swelling data.

The strength of the van der Waals interaction is proportional to the net dielectric contrast between lipids and solvent: the larger the contrast, the stronger the attraction between adjacent bilayers (47). To understand how this dielectric contrast is modified by salt, we distinguish between static (low-frequency) and optical (high-frequency) dielectric responses of lipid-salt multilayers (50). Static values are modified by a spatial redistribution of ions, whereas optical values are modified by ionic polarization in response to spontaneous charge fluctuations. Screening at low frequency is responsible for a 50% decrease in the van der Waals attraction for both KCl and KBr. The enhanced swelling in the presence of KBr compared with KCl at low salt (Figs. 1, 2) is attributable to electrostatic repulsion from the binding of Br^- ions (51). This electrostatic force, however, becomes negligible in 1 M salt, at which the screening length is <3 Å.

With weakened attraction, the net free energy of the multilamellar stacking increases. From this perspective, partitioning of salt between bilayers is energetically unfavorable. For a given salt concentration in the bath, the final equilibrium spacing is established by the gain in ion-mixing entropy acting against the weakened bilayer attraction. Consider a fully hydrated, equilibrated MLV in water introduced into a salt solution, as illustrated in **Fig. 7A**. Entropy favors partitioning of salt into the interlamellar space. Keeping the interlamellar water clear of salt in the presence of 1 M salt in the bath requires an osmotic penalty $\Delta G_1 \approx 1.2\ k_B T$/lipid. As salt enters to gain mixing entropy, van der Waals attraction is weakened (Fig. 7B). This causes the membranes to move to a new equilibrium point at greater spacing (Fig. 7C). To hold the original spacing would increase the energy to $-\Delta G_2 \approx 2.5 \times 10^{-3}\ k_B T$/lipid, as calculated from the pressure curves in Fig. 6.

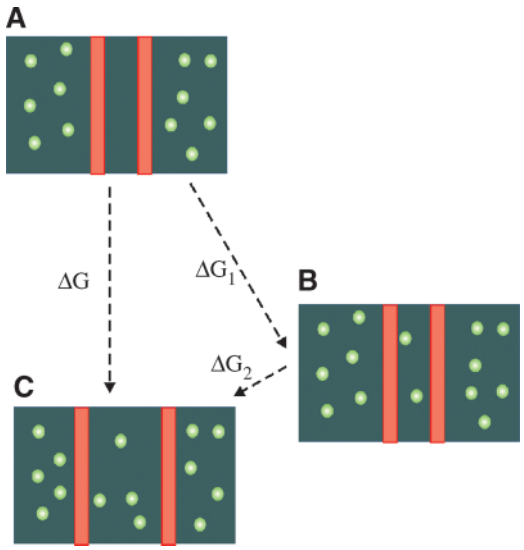

Fig. 7. Conceptual drawing of various energy contributions to multilayer swelling with added salt. Excluding salt from the interlamellar (central) region incurs an entropic cost (A), providing a driving force for the permeation of salt inside multilamellar vesicles (B). This provides an entropic gain but incurs an energetic penalty as a result of weakened van der Waals attraction. A new equilibrium separation is reached (C) at which the net free energy, including mixing entropy and stack energy, are balanced.

Beyond these considerations of forces between bilayers, interfacial distribution of salt is determined by the competition between salt and lipid head groups for interlamellar water. As determined by neutral buoyancy measurements (51), salt concentration inside the MLVs is significantly lower than in the bulk. This is explained by a large number of water molecules tightly bound to the lipid head groups and thus unavailable to solvate salt ions. Salt is excluded from the vicinity of PC head groups, with the "sticky" Br^- being less excluded than Cl^-.

At the cellular level, specific ionic effects have been recognized primarily for osmoregulation mechanisms (4) and growth rates of halophilic bacteria (2). Here, we suggest that quantifying the nonnegligible effect of salt on lipid interaction will help elucidate such cellular membrane mechanisms.

The authors thank Joel Cohen, Per Hansen, and Rudi Podgornik for many stimulating discussions on interbilayer interactions. This research was supported by the Intramural Research Program of the National Institutes of Health, National Institute of Child Health and Human Development. Funding for the Carnegie Mellon University effort was provided by National Institutes of Health Grant GM-44976-11 (PI = J.F.N.). For data from oriented samples, X-ray beamtime at the Cornell High-Energy Synchrotron Source (National Science Foundation Grant DMR-0225180) is gratefully acknowledged.

REFERENCES

1. Reynolds, J. A. 1972. Are inorganic cations essential for stability of biological membranes? *Ann. N. Y. Acad. Sci.* **195:** 75–85.
2. Lo Nostro, P., B. W. Ninham, A. Lo Nostro, G. Pesavento, L. Fratoni, and P. Baglioni. 2005. Specific ion effects on the growth rates of *Staphylococcus aureus* and *Pseudomonas aeruginosa*. *Phys. Biol.* **2:** 1–7.
3. Keppler, F., R. Eiden, V. Niedan, J. Pracht, and H. F. Scholer. 2000. Halocarbons produced by natural oxidation processes during degradation of organic matter. *Nature.* **403:** 298–301.
4. Poolman, B., J. J. Spitzer, and J. A. Wood. 2004. Bacterial osmosensing: roles of membrane structure and electrostatics in lipid-protein and protein-protein interactions. *Biochim. Biophys. Acta.* **1666:** 88–104.
5. Grigorjev, P. A., and S. M. Bezrukov. 1994. Hofmeister effect in ion transport: reversible binding of halide anions to the roflamycoin channel. *Biophys. J.* **67:** 2265–2271.
6. Rand, R. P., and V. A. Parsegian. 1989. Hydration forces between phospholipid bilayers. *Biochim. Biophys. Acta.* **988:** 351–376.
7. McDaniel, R. V., T. J. McIntosh, and S. A. Simon. 1983. Nonelectrolyte substitution for water in phosphatidylcholine bilayers. *Biochim. Biophys. Acta.* **731:** 97–108.
8. McIntosh, T. J., and S. A. Simon. 1993. Contributions of hydration and steric (entropic) pressures to the interactions between phosphatidylcholine bilayers: experiments with the subgel phase. *Biochemistry.* **32:** 8374–8384.
9. Nagle, J. F., and S. Tristram-Nagle. 2000. Structure of lipid bilayers. *Biochim. Biophys. Acta.* **1469:** 159–195.
10. Korreman, S. S., and D. Posselt. 2001. Modification of anomalous swelling in multilamellar vesicles induced by alkali halide salts. *Eur. Biophys. J.* **30:** 121–128.
11. Deme, B., M. Dubois, and T. Zemb. 2002. Swelling of a lecithin lamellar phase induced by small carbohydrate solutes. *Biophys. J.* **82:** 215–225.
12. Gottlieb, M. H., and E. D. Eanes. 1972. Influence of electrolytes on thicknesses of phospholipid bilayers of lamellar lecithin mesophases. *Biophys. J.* **12:** 1533–1539.
13. Chapman, D., W. E. Peel, B. Kingston, and T. H. Lilley. 1977. Lipid phase transitions in model biomembranes. The effect of ions on phosphatidylcholine bilayers. *Biochim. Biophys. Acta.* **464:** 260–275.
14. Cunningham, B. A., J. E. Shimotake, W. Tamuralis, T. Mastran, W. M. Kwok, J. W. Kauffman, and L. J. Lis. 1986. The influence of ion species on phosphatidylcholine bilayer structure and packing. *Chem. Phys. Lipids.* **39:** 135–143.
15. Cunningham, B. A., and L. J. Lis. 1989. Interactive forces between phosphatidylcholine bilayers in monovalent salt solutions. *J. Colloid Interface Sci.* **128:** 15–25.
16. Simon, S. A., and T. J. McIntosh. 1989. Magnitude of the solvation pressure depends on dipole potential. *Proc. Natl. Acad. Sci. USA.* **86:** 9263–9267.
17. Tristram-Nagle, S., and J. F. Nagle. 2004. Lipid bilayers: thermodynamics, structure, fluctuations, and interactions. *Chem. Phys. Lipids.* **127:** 3–14.
18. Liu, Y., and J. F. Nagle. 2004. Diffuse scattering provides material parameters and electron density profiles of biomembranes. *Phys. Rev. E.* **69:** 40901.
19. Kučerka, N., Y. F. Liu, N. J. Chu, H. I. Petrache, S. Tristram-Nagle, and J. F. Nagle. 2005. Structure of fully hydrated fluid phase DMPC and DLPC lipid bilayers using X-ray scattering from oriented multilamellar arrays and from unilamellar vesicles. *Biophys. J.* **88:** 2626–2637.
20. Brown, M. F., and J. Seelig. 1977. Ion-induced changes in head group conformation of lecithin bilayers. *Nature.* **269:** 721–723.
21. Eisenberg, M., T. Gresalfi, T. Riccio, and S. McLaughlin. 1979. Adsorption of monovalent cations to bilayer membranes containing negative phospholipids. *Biochemistry.* **18:** 5213–5223.
22. Tatulian, S. A. 1987. Binding of alkaline-earth metal cations and some anions to phosphatidylcholine liposomes. *Eur. J. Biochem.* **170:** 413–420.
23. Cohen, J. A. 1995. Electrophoretic characterization of liposomes. *Methods Enzymol.* **367:** 148–176.
24. Aroti, A., E. Leontidis, E. Maltseva, and G. Brezesinski. 2004. Effects of Hofmeister anions on DPPC Langmuir monolayers at the air-water interface. *J. Phys. Chem. B.* **108:** 15238–15245.
25. Rappolt, M., K. Pressl, G. Pabst, and P. Laggner. 1998. Lα-phase separation in phosphatidylcholine-water systems induced by alkali chlorides. *Biochim. Biophys. Acta.* **1372:** 389–393.
26. Gruner, S. M., R. P. Lenk, A. S. Janoff, and M. J. Ostro. 1985. Novel multilayered lipid vesicles: comparison of physical characteristics of multilamellar liposomes and stable plurilamellar vesicles. *Biochemistry.* **24:** 2833–2842.
27. Tatulian, S. A. 1983. Effect of lipid phase transition on the binding of anions to dimyristoylphosphatidylcholine liposomes. *Biochim. Biophys. Acta.* **736:** 189–195.
28. Tatulian, S. A., V. I. Gordeliy, A. E. Sokolova, and A. G. Syrykh. 1991. A neutron diffraction study of the influence of ions on phospholipid membrane interactions. *Biochim. Biophys. Acta.* **1070:** 143–151.
29. Peitzsch, R. M., M. Eisenberg, K. A. Sharp, and S. McLaughlin. 1995. Calculations of the electrostatic potential adjacent to model phospholipid bilayers. *Biophys. J.* **68:** 729–738.
30. Rydall, J. R., and P. M. Macdonald. 1992. Investigation of anion binding to neutral lipid membranes using 2H NMR. *Biochemistry.* **31:** 1092–1099.
31. Clarke, R. J., and C. Lupfert. 1999. Influence of anions and cations on the dipole potential of phosphatidylcholine vesicles: a basis for the Hofmeister effect. *Biophys. J.* **76:** 2614–2624.
32. Tristram-Nagle, S., R. Zhang, R. M. Suter, C. R. Worthington, W. J. Sun, and J. F. Nagle. 1993. Measurement of chain tilt angle in fully hydrated bilayers of gel phase lecithins. *Biophys. J.* **64:** 1097–1109.
33. Zhang, R. T., R. M. Suter, and J. F. Nagle. 1994. Theory of the structure factor of lipid bilayers. *Phys. Rev. E.* **50:** 5047–5060.
34. Lyatskaya, Y., Y. F. Liu, S. Tristram-Nagle, J. Katsaras, and J. F. Nagle. 2001. Method for obtaining structure and interactions from oriented lipid bilayers. *Phys. Rev. E.* **63:** 011907.
35. Wiener, M. C., R. M. Suter, and J. F. Nagle. 1989. Structure of the fully hydrated gel phase of dipalmitoylphosphatidylcholine. *Biophys. J.* **55:** 315–325.
36. Nagle, J. F., and M. C. Wiener. 1988. Structure of fully hydrated bilayer dispersions. *Biochim. Biophys. Acta.* **942:** 1–10.
37. Nagle, J. F., and M. C. Wiener. 1989. Relations for lipid bilayers. Connection of electron density profiles to other structural quantities. *Biophys. J.* **55:** 309–313.

38. Nagle, J. F., and D. A. Wilkinson. 1978. Lecithin bilayers. Density measurements and molecular interactions. *Biophys. J.* **23:** 159–175.
39. Wiener, M. C., S. Tristram-Nagle, D. A. Wilkinson, L. E. Campbell, and J. F. Nagle. 1988. Specific volumes of lipids in fully hydrated bilayer dispersions. *Biochim. Biophys. Acta.* **938:** 135–142.
40. Apelblat, A., and E. Manzurola. 1999. Volumetric properties of water, and solutions of sodium chloride and potassium chloride at temperatures from T=277.15 K to T=343.15 K at molalities of (0.1, 0.5, and 1.0) mol/kg. *J. Chem. Thermodyn.* **31:** 869–893.
41. Landolt-Bornstein, H. H. 1971. Physikalisch-Chemische Tabellen, Eigenschaften der Materie in Ihren Aggregatzustanden. Springer-Verlag, Berlin.
42. Petrache, H. I., S. W. Dodd, and M. F. Brown. 2000. Area per lipid and acyl length distributions in fluid phosphatidylcholines determined by H^2 NMR spectroscopy. *Biophys. J.* **79:** 3172–3192.
43. Chapman, C. J., W. L. Erdahl, R. W. Taylor, and D. R. Pfeiffer. 1990. Factors affecting solute entrapment in phospholipid vesicles prepared by the freeze-thaw extrusion method: a possible general method for improving the efficiency of entrapment. *Chem. Phys. Lipids.* **55:** 73–83.
44. Chu, N., N. Kučerka, Y. F. Liu, S. Tristram-Nagle, and J. F. Nagle. 2005. Anomalous swelling of lipid bilayer stacks is caused by softening of the bending modulus. *Phys. Rev. E.* **71:** 041904.
45. Petrache, H. I., N. Gouliaev, S. Tristram-Nagle, R. T. Zhang, R. M. Suter, and J. F. Nagle. 1998. Interbilayer interactions from high-resolution x-ray scattering. *Physical Review E.* **57:** 7014–7024.
46. Rawicz, W., K. C. Olbrich, T. McIntosh, D. Needham, and E. Evans. 2000. Effect of chain length and unsaturation on elasticity of lipid bilayers. *Biophys. J.* **79:** 328–339.
47. Parsegian, V. A., and B. W. Ninham. 1969. Application of Lifshitz theory to the calculation of van der Waals forces across thin lipid films. *Nature.* **224:** 1197–1198.
48. Helfrich, W. 1978. Steric interaction of fluid membranes in multilayer systems. *Z. Naturforsch.* **33:** 305–315.
49. Parsegian, V. A. 1975. Long range van der Waals forces. Theorex, La Jolla, CA.
50. Parsegian, V. A., and G. H. Weiss. 1981. Spectroscopic parameters for computation of van der Waals forces. *J. Colloid Interface Sci.* **81:** 285–289.
51. Petrache, H. I., I. Kimchi, D. Harries, and V. A. Parsegian. 2005. Measured depletion of ions at the biomembrane interface. *J. Am. Chem. Soc.* **127:** 11546–11547.